

an indicator of interannual variability in thaw depth is uncertain because placement of the probes may have disturbed the local conditions, one of the sites was disturbed by the installation of ancillary equipment in 1995, and the horizontal distribution of soil frost may have varied from year to year.

28. A uniform 2.5°C increase in temperature would in-

crease the annual number of sunlit hours on days with mean temperatures above freezing by ~8%. The length of the growing season at Harvard Forest, where warming in spring is more gradual and the growing season is shorter because the forest is deciduous, is more sensitive to warming (5, 14).

29. This work was supported by the U.S. National Aero-

navics and Space Administration. We thank the BOREAS science team; the BOREAS support staff; and especially P. Sellers, F. Hall, K. Spence, D. Hodgkinson, B. Lesley, R. Mendelson, A. Dunn, and M. Pender.

26 August 1997; accepted 12 November 1997

## Evidence of Shallow Fault Zone Strengthening After the 1992 M7.5 Landers, California, Earthquake

Yong-Gang Li,\* John E. Vidale, Keiiti Aki, Fei Xu, Thomas Burdette

Repeated seismic surveys of the Landers, California, fault zone that ruptured in the magnitude (*M*) 7.5 earthquake of 1992 reveal an increase in seismic velocity with time. *P*, *S*, and fault zone trapped waves were excited by near-surface explosions in two locations in 1994 and 1996, and were recorded on two linear, three-component seismic arrays deployed across the Johnson Valley fault trace. The travel times of *P* and *S* waves for identical shot-receiver pairs decreased by 0.5 to 1.5 percent from 1994 to 1996, with the larger changes at stations located within the fault zone. These observations indicate that the shallow Johnson Valley fault is strengthening after the main shock, most likely because of closure of cracks that were opened by the 1992 earthquake. The increase in velocity is consistent with the prevalence of dry over wet cracks and with a reduction in the apparent crack density near the fault zone by approximately 1.0 percent from 1994 to 1996.

A fault plane undergoes sudden stresses, shaking, and cracking during an earthquake. Extensive research has been directed toward understanding this phenomenon (1, 2), but many facets remain obscure.

We focus on the rate at which a fault regains its strength following a large earthquake. This rate is needed to understand how fault zones strengthen or "heal" after an earthquake, but so far, only simple laws have been assumed based on laboratory experiments rather than direct observations in the field. In addition, the healing rate may affect the probability of another earthquake in a fault zone. Experimental studies (3) indicate that a longer interval since the previous episode of faulting correlates with higher stress drop in the subsequent rupture. Studies of repeated earthquakes along a fault (4) show trends that are consistent with state- and rate-dependent healing models (5).

We had the particularly favorable situation of probing the evolution of a shallow

fault that had recently undergone large displacements. Earlier efforts to identify dilatancy that might be detectable near fault zones failed because of low sensitivity coupled with what we now know to be subtle precursory changes due to dilatancy (2, 6). Repeated surveys near Parkfield (7) is showing small changes in velocity over time, but in the absence of a large earthquake and with uncertainty about the precise location of the velocity change, its significance is hard to assess. A comparison of earthquakes before and after a specific large event showed a small coseismic reduction in wave velocity at stations with unconsolidated sedimentary rocks that were strongly shaken (8), suggesting the temporal change was a shallow effect of shaking rather than a physical change in the bedrock. One study (9) suggests changes in scattering of *P* waves with a 1-s period around the time of large earthquakes, but the pattern is not yet well established.

We conducted two identical seismic experiments on 2 November 1994 and 6 August 1996 (Fig. 1) to monitor the change of fault zone physical properties after the 1992 M7.5 Landers earthquake. A pair of explosions, or "shots," in 30-m boreholes along the Johnson Valley fault segment of the Landers fault zone were detonated in each experiment, using 400 to 700 pounds of chemical emulsions for each. A pair of lin-

ear three-component seismic arrays recorded the arrivals of seismic waves for each explosion. The arrays were 3-km in length and aligned perpendicular to the fault. The two arrays were separated by 13 km, and the explosions were located between the arrays (Fig. 1). The array along line 1 had 36 stations and the array along line 3 had 21 stations.

Line 1 is centered at the region that experienced the maximum amount of slip—about 3 m—on the Johnson Valley fault during the Landers earthquake (Fig. 1). Slip is smaller near line 3, and also diminished to the north until the surface rupture connected with the Homestead Valley fault. Fault slip at depth is more difficult to determine, but seems to resemble the slip at the surface (10). The recurrence of faulting on the Johnson Valley fault is estimated to exceed 1000 years (11, 12).

The data from line 3, collected in 1996, had *P* waves visible on all traces near 1 s. The *S* waves had a longer period and were more prominent on the horizontal components near 2 s, and the fault zone trapped modes appeared from 3 to 8 s (Fig. 2). The trapped waves showed larger amplitudes,

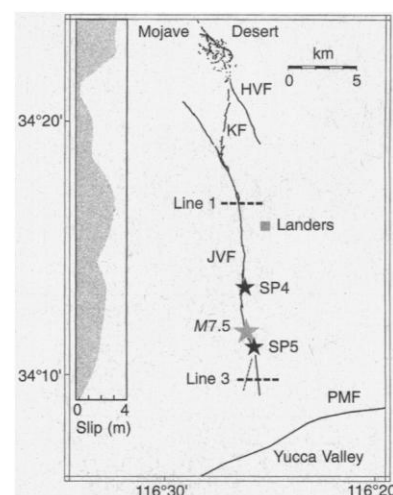


**Fig. 1.** Map of the study region showing locations of two seismic arrays at line 1 and line 3 and two explosions SP4 and SP5 in the fault zone of the 1992 Landers, California, earthquake. Only the southern half of the Landers rupture lies within this map, and the dextral surface-fault slip profile is shown (inset) to the left of the map (12). JVF, Johnson Valley fault; KF, Kickapoo fault; HVF, Homestead Valley fault; and PMF, Pinto Mountain fault.

Y.-G. Li and K. Aki, Department of Earth Sciences, University of Southern California, Los Angeles, CA 90089-0740, USA.

J. E. Vidale and F. Xu, Department of Earth and Space Sciences, University of California at Los Angeles, Los Angeles, CA 90095-1567, USA.

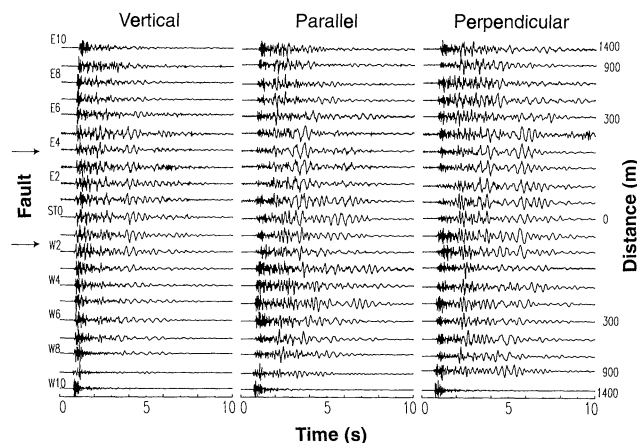
T. Burdette, U.S. Geological Survey, Menlo Park, CA 94025, USA.

\*To whom correspondence should be addressed. E-mail: ygli@terra.usc.edu

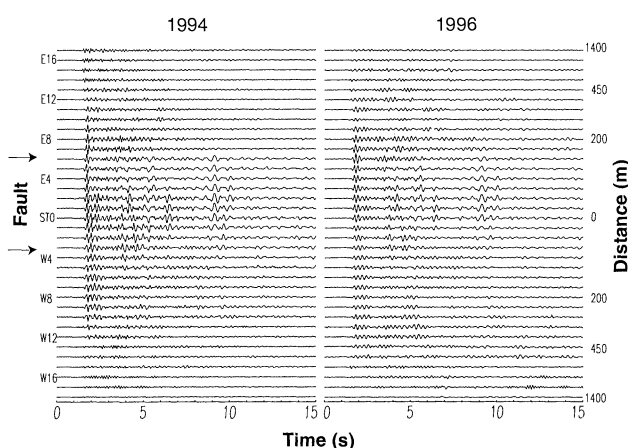
lower frequencies, and longer wavetrains with slight dispersion than *P* and *S* waves. However, the trapped waves were not visible on stations located further than 200 m

from the fault trace. The fault zone trapped waves excited by near-surface explosions are similar to those generated by microearthquakes occurring within the fault zone

**Fig. 2.** Three-component seismograms recorded along line 3 from shot SP5 in 1996. The REFTEK seismometers recorded continuously, and time was synchronized by global positioning system. The sensors, Mark product L22, were buried with the three components aligned vertical, parallel, and perpendicular to the fault trace. Station spacing is not even; 12 stations located closest to the fault trace have 50-m spacing, but there is 100- to 500-m spacing for farther stations.



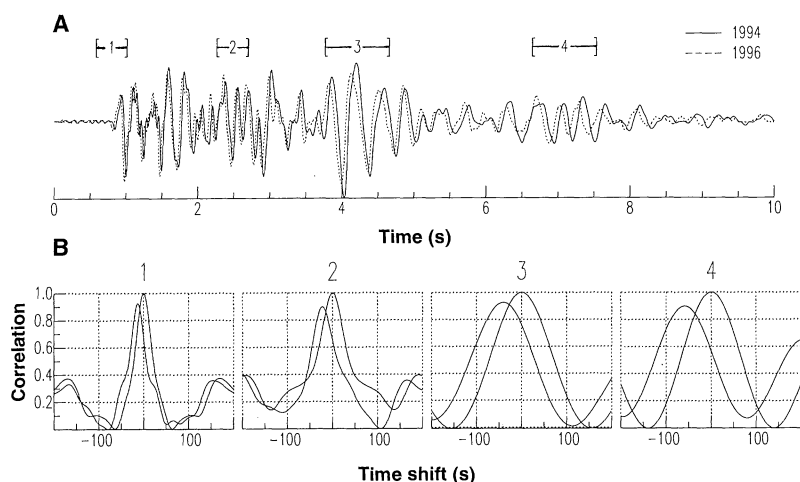
**Fig. 3.** Vertical component of line 1 for shot 4 in 1994 and 1996. Station spacing is not even; 16 stations located closest to the fault trace have 25-m spacing, but there is 50- to 250-m spacing for farther stations. Seismograms are low-pass filtered at 8 Hz and plotted with a fixed-amplitude scale for all traces.



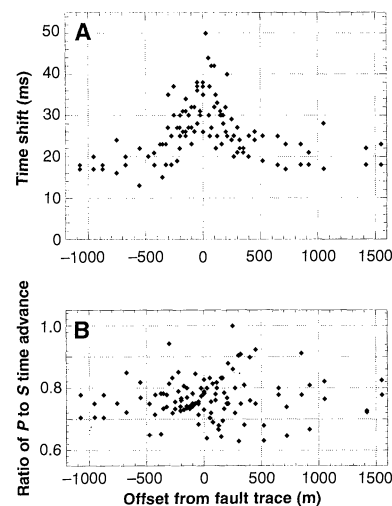
at Landers (13), but have lower frequencies and travel more slowly, suggesting that the fault zone is seismically slower and possibly wider as it approaches the surface. We have used microearthquake-generated trapped waves recorded at the Landers fault zone to delineate a 180-m-wide fault core where *S* velocity is reduced by 30 to 50% at the seismogenic depth (13). We, however, will focus on the temporal variations in arrival times of *P* and *S* waves that travel through the shallow fault zone.

Figure 3 shows the similar wave forms of *P*, *S*, and trapped waves recorded on line 1 from shot SP4 between 1994 and 1996, but with a time advance  $<0.1$  s for the 1996 recordings. For an example, the travel time decreases of these waves in 1996 are shown more clearly in Fig. 4. We extracted *P*, *S*, and trapped waves from four time windows and cross-correlated each pair of recordings for the same shot and same seismometer to obtain time differences between the 1994 and 1996 recordings. Windows 1 and 2 are *P* and *S* waves, respectively. Windows 3 and 4 are some sort of fault zone trapped waves. All phases arrived faster in 1996 than in 1994. Although the travel times of these waves decreased only a few hundredths of a second from 1994 to 1996, the changes are an order of magnitude larger than the uncertainty in the origin time of the explosion, which is less than 0.001 s. Also note that the peaks of the cross-correlation are near 1, indicating waveform similarity between 1994 and 1996.

The ratio of decrease in travel time for *P* to *S* waves ( $\Delta t_P/\Delta t_S$ ) between 1994 and 1996 is 0.77. This is from 112 measurements, with an SD of 0.07 (Fig. 5). This



**Fig. 4.** (A) Vertical component seismograms recorded at station W1 of line 3 for shot SP5 in 1994 (solid lines) and in 1996 (dotted lines). (B) Autocorrelations and cross-correlations of seismograms recorded in 1994 and 1996 at the same stations for four time windows including *P* (window 1), *S* (window 2), and fault zone trapped waves (windows 3 and 4). The length of windows 1 and 2 is 0.5 s, whereas the length of windows 3 and 4 is 1 s. The peak of the autocorrelation curve is at zero time in each window. The negative time shift indicates time advance. The cross-correlations in windows 1 to 4 reveal time advances of 0.018, 0.025, 0.045, and 0.06 s, respectively, for the waves in 1996.



**Fig. 5.** (A) Arrival-time advances of *S* waves in 1996 determined from cross-correlations of three-component recordings. (B) Ratio of time advances measured for *P* waves divided by time advances for *S* waves.

ratio is valid for all  $P$  and  $S$  arrivals both within and outside the fault zone. Also, the arrivals in the middle of the linear arrays (near the fault trace) have a greater time advance from 1994 to 1996 than the arrivals at stations toward the edges of the arrays. Based on the size of the zone exhibiting larger arrival time decreases from 1994 to 1996 (Fig. 5), we estimated that the fault zone in the top few kilometers is about 300 m wide.

If the change in velocity is uniform through the crust that is sampled by these waves, the decrease in travel times (for example, in Fig. 4) would be easy to interpret. The  $P$  wave arrives 0.01 s earlier, with a travel time of 1 s, so the  $P$  wave velocity increased by 1%. Similarly, the  $S$  wave arrives 0.025 s earlier, with a travel time of 2.5 s, so the  $S$  wave velocity also increased by 1%. The trapped waves with longer travel times have larger time advances than do  $P$  and  $S$  waves, again resulting in  $\sim 1\%$  increase in velocity.

The decrease in the travel time of these waves is largest within the fault zone (Fig. 5). Also, the longer ray paths show the larger travel time changes. However, the change is not proportional to travel distance. The longest path is 10 km (shot SP5 to line 1) and the shortest path is 3 km (shot SP5 to line 3), but the time advance for the 10-km path is only 20 to 30% larger than the time advance for the 3-km path. Lateral variations in time advance along the fault are also evident, as the pair of shot SP4 and line 3 shows greater time advances than the pair of shot SP4 and line 1, despite their similar path lengths. These trends suggest that the velocity change is strongest in the fault zone rather than being distributed uniformly across the fault zone and the bedrock on both sides and that the velocity change is less in the deeper part of the fault zone. The deeper ray paths penetrate 2 to 3 km below the surface (14).

The increase in the velocity of  $P$  and  $S$  waves with time is most likely due to the closure of dry cracks as the crust heals after the earthquake. This process may be thought of as the reductive dilatancy (2, 6). Estimates of the change in velocity due to the change in the density of cracks may be calculated (15). We assumed randomly oriented cracks, although there may be some alignment, whose coherence is not simple to predict and may change with time. Dry cracks in a Poisson solid are predicted to cause  $\Delta t_p/\Delta t_s$  of  $\sim 1.22$ . Water-filled cracks, on the other hand, cause  $\Delta t_p/\Delta t_s$  of only  $\sim 0.27$ . So the observed  $\Delta t_p/\Delta t_s \sim 0.77$  (Fig. 5) is closer to the prediction for dry cracks. If the rock has an anomalous Poisson's ratio such that the  $P$  wave velocity is twice the  $S$  wave velocity, then  $\Delta t_p/\Delta t_s$  is expected to

be 1.64 for dry cracks and 0.17 for wet cracks.

Because the observed ratio is lower than the predicted ratio for dry cracks, some fluid may be present in the cracks. Also, the apparent density of saturated cracks may decrease more slowly or quickly than the density of dry cracks immediately after an earthquake, but the simplest interpretation is the prevalence of dry rather than wet cracks.

A 1% increase in the seismic velocities is expected from a roughly 1% decrease in the apparent crack density (15). Apparent crack density is defined as  $a^3 N/v$ , where  $N/v$  is the number of cracks per unit volume and  $a$  is the radius of penny-shaped cracks. Because the cracks are thin, the reduction in apparent crack density by 1% causes a reduction in volume that is much less than 1%.

Seismic velocities would increase if the water level rose. However, a change in the water table would not produce the signal that we saw. In detail, if a layer that was previously unsaturated had become saturated during the postearthquake period, shear and compressional velocities would indeed increase. However, this would slightly increase the  $S$  wave velocity of the layer, but greatly increase the  $P$  wave velocity, in disagreement with the similar  $S$  and  $P$  velocity increases observed. In addition, an implausibly large change in water level of more than 200 m is needed to change travel time by 0.02 s, as observed.

The reduction in apparent crack density might be discernible in geodetic measurements. As rocks heal, there might be either more of the right-lateral shear deformation from the regional stress field that dominated the coseismic displacements or fault-normal compression from the reduction in volume. Deformation has been reported with a time scale of several years and a distribution pattern matching the Landers mainshock double couple (16). One pattern observed is not explained by our model; synthetic aperture radar images reveal uplift and depression with a 1-year time scale that is consistent with reequilibration of pore fluids because of mainshock-induced stresses (17). We are not aware of any reports of fault-normal contraction for the Landers fault zone. For the 1989 Loma Prieta earthquake, however, there is evidence of fault-normal contraction of several centimeters per year in the years following the event (18).

We conclude that some cracks that had opened during the mainshock closed soon thereafter. The closure of cracks 2 to 4 years after the earthquake is consistent with our tentative interpretation of the strong, low-velocity Landers fault zone waveguide as

being at least partially created during the mainshock (13). Closure of cracks would increase the frictional strength of the fault zone, as well as its stiffness (19). Thus, such a pattern of healing fault zones may help explain observations of increasing stress drop with increasing recurrence intervals (3, 4).

## REFERENCES AND NOTES

1. K. Aki, *Tectonophysics* **13**, 423 (1972); C. H. Scholz, N. H. Dawers, J.-Z. Yu, M. H. Anders, P. A. Cowei, *J. Geophys. Res.* **98**, 21951 (1993); J. H. Dieterich, *ibid.* **84**, 2161 (1979); *ibid.*, p. 2169; J. R. Rice, *ibid.* **98**, 9885 (1993); R. L. Kranz and C. H. Scholz, *ibid.* **82**, 4893 (1977); W. D. Mooney and A. Ginzburg, *Pure Appl. Geophys.* **124**, 141 (1986).
2. C. H. Scholz, *The Mechanics of Earthquakes and Faulting* (Cambridge Univ. Press, New York, 1990).
3. H. B. Houston, *Geophys. Res. Lett.* **17**, 1021 (1990); H. Kanamori and C. R. Allen, in *Earthquake Source Mechanics*, S. Das et al., Eds. (Geophysical Monograph **37**, American Geophysical Union, Washington, DC, 1986), pp. 227–236; C. H. Scholz, C. A. Aviles, S. G. Wesnousky, *Bull. Seismol. Soc. Am.* **76**, 65 (1986).
4. C. J. Marone, J. E. Vidale, W. L. Ellsworth, *Geophys. Res. Lett.* **22**, 3095 (1995); J. E. Vidale, W. L. Ellsworth, A. Cole, C. J. Marone, *Nature* **368**, 624 (1994).
5. J. H. Dieterich, *J. Geophys. Res.* **77**, 3690 (1972).
6. A. Nur, *Bull. Seismol. Soc. Am.* **62**, 1217 (1972); C. H. Scholz, *Science* **201**, 441 (1978).
7. E. Karageorgi, T. V. McEvilly, R. Clymer, *Bull. Seismol. Soc. Am.* **87**, 39 (1997).
8. D. A. Dodge and G. C. Beroza, *J. Geophys. Res.* **102**, 24437 (1997).
9. J. Revenaugh, *Science* **270**, 1344 (1995).
10. B. P. Cohee and G. C. Beroza, *Bull. Seismol. Soc. Am.* **84**, 692 (1994); D. J. Wald and T. H. Heaton, *ibid.*, p. 668.
11. M. Herzberg and T. Rockwell, *Eos (Fall Suppl.)* **74** (no. 43), 612 (1993); C. R. Rubin and K. Sieh, *J. Geophys. Res.* **102**, 15319 (1997).
12. K. Sieh et al., *Science* **260**, 171 (1993).
13. Y. G. Li, K. Aki, D. Adams, A. Hasemi, W. H. K. Lee, *J. Geophys. Res.* **99**, 11705 (1994); Y. G. Li, J. E. Vidale, K. Aki, C. J. Marone, W. H. K. Lee, *Science* **265**, 367 (1994).
14. H. Magistrale, H. Kanamori, C. Jones, *J. Geophys. Res.* **97**, 14115 (1992); J. Mori and D. Helmberger, *Bull. Seismol. Soc. Am.* **86**, 1845 (1996).
15. H. D. Garbin and L. Knopoff, *Quart. Appl. Math.* **30**, 453 (1973); *ibid.* **32**, 296 (1975a); *ibid.* (1975b), p. 301.
16. Y. S. Bock et al., *J. Geophys. Res.* **102**, 18013 (1997); Z. K. Shen, D. D. Jackson, B. X. Ge, *ibid.* **101**, 27957 (1996).
17. G. Peltzer, P. Rosen, F. Rogez, K. Hudnut, *Science* **273**, 1202 (1996).
18. R. Burgmann, P. Segall, M. Lisowski, J. Svarc, *J. Geophys. Res.* **102**, 4933 (1997); J. C. Savage, M. Lisowski, J. L. Svarc, *ibid.* **99**, 13757 (1994).
19. C. Marone, *Nature*, in press; C. Marone, in preparation.
20. Supported by NSF grant EAR-9404762 and the Southern California Earthquake Center under NSF grant EAR-8920136 and U.S. Geological Survey grant 14-0A-0001-A0899. We appreciate D. Adams, S. Arturo, D. Bowman, G. Ely, K. Favret, M. Forrest, A. Martin, J. Wedberg, and A. Wei for their work in the field. We thank the U.S. Bureau of Land Management at Barstow, CA, and many land property owners at Landers, including E. Landau and R. Hawley for their permission to carry out the experiment in the public and private lands. We acknowledge the support of the IRIS-PASSCAL Instrument Center for the use of their instruments.

1 October 1997; accepted 26 November 1997